Microbiota-Derived Indole Metabolites Promote Human and Murine Intestinal Homeostasis through Regulation of Interleukin-10 Receptor

Alexeev, E. E., Lanis, J. M., Kao, D. J., Campbell, E., Kelly, C. J., Battista, K. D., Gerich, M. E., Jenkins, B. R., Walk, S. T., Kominsky, D. J., & Colgan, S. P. (2018). Microbiota-Derived Indole Metabolites Promote Human and Murine Intestinal Homeostasis through Regulation of Interleukin-10 Receptor. *The American journal of pathology*, *188*(5), 1183-1194. https://doi.org/10.1016/j.ajpath.2018.01.011

Published in:
The American journal of pathology

Document Version:
Peer reviewed version

Microbiota-derived indole metabolites promote human and murine intestinal homeostasis through regulation of interleukin-10 receptor

Short title: Indole metabolites and intestinal homeostasis

Erica E. Alexeev[1], Jordi M. Lanis[1], Daniel J. Kao[1], Eric L. Campbell[2], Caleb J. Kelly[1], Kayla D. Battista[1], Mark E. Gerich[1], Brittany R. Jenkins[3], Seth T. Walk[3], Douglas J. Kominsky[3#], Sean P. Colgan[1#]

[1]*Mucosal Inflammation Program and Department of Medicine, University of Colorado, Anschutz Medical Campus, Aurora, CO*

[2]*Centre for Experimental Medicine, Queen's University Belfast, Belfast, BT97BL, Northern Ireland, UK*

[3]*Department of Microbiology and Immunology, Montana State University, Bozeman, MT*

[#]*Co-senior authors*

Funding: This work was supported by NIH grants DK1047893, DK50189, DK095491, DK103639, DK103712 and VA Merit BX002182. Funding for generating and maintaining the human intestinal organoids was provided by the Bill and Melinda Gates Foundation.

Correspondence to: Sean Colgan, Mucosal Inflammation Program, University of Colorado, Anschutz Medical Campus, 12700 East 19th Ave. MS B-146, Aurora, CO 80045, USA. Office phone: 303-724-7235 Fax: 303-724-7243
E-mail: sean.colgan@ucdenver.edu
or
Douglas Kominsky, Department of Microbiology and Immunology, Montana State University, 109 Lewis Hall, Bozeman, MT 59717, USA. Office phone: 406-994-5667 Fax: 406-994-4926
E-mail: douglas.kominsky@montana.edu

Competing interests: The authors declare that no conflict of interests exists.

Abstract

Interactions between the gut microbiota and the host are important for health, where dysbiosis has emerged as a likely component of mucosal disease. The specific constituents of the microbiota that contribute to mucosal disease are not well defined. We sought to define microbial components that regulate homeostasis within the intestinal mucosa. Using an unbiased, metabolomic profiling approach, we identified a selective depletion of indole and indole-derived metabolites in murine and human colitis. We demonstrated that indole-3-propionic acid (IPA) was selectively diminished in circulating serum from human subjects with active colitis and that IPA served as a biomarker of disease remission. Administration of indole metabolites showed prominent induction of IL-10R1 on cultured intestinal epithelia that was explained by activation of the aryl hydrocarbon receptor (AHR). Colonization of germ-free mice with wild-type *E. coli*, but not *E. coli* mutants unable to generate indole, induced colonic epithelial IL-10R1. Moreover, oral administration of IPA significantly ameliorated disease in a chemically-induced murine colitis model. This work defines a novel role of indole metabolites in anti-inflammatory pathways mediated by epithelial IL-10 signaling and identifies possible avenues for utilizing indoles as novel therapeutics in mucosal disease.

Keywords: indole; microbiota; colitis; mucosal homeostasis

Introduction

The mammalian gastrointestinal (GI) tract plays host to trillions of microbes, collectively termed the microbiota, where a critical mutualism exists within the intestinal mucosa. The microbiota contributes significantly to gut homeostasis but can also contribute to establishing and maintaining mucosal disease [1]. Intestinal mucosal surfaces act as primary barriers to microbial invasion, where commensal bacteria work in a dynamic and intimate interaction with the gut epithelium and influence host cellular and immune responses [2]. Inflammatory bowel disease (IBD) is a chronic inflammatory disease of the GI tract that is comprised of Crohn's disease (CD) and ulcerative colitis (UC). It is known that IBD is caused by interactions between genetic and environmental factors, and results in perturbations of the microbiota, though precisely how microbial factors affect gut homeostasis and immune response have not been extensively explored [3-5].

The significance of IL-10 signaling is well established in IBD. This anti-inflammatory cytokine, which signals through the IL-10 receptor ligand-binding subunit (IL-10R1), is induced during inflammation and attenuates excessive production of pro-inflammatory mediators in various cell types, including intestinal epithelial cells (IEC) [6, 7]. Functional IL-10 signaling is associated with enhanced mucosal barrier function and results in maintenance and homeostasis of the epithelia [7]. Previous work, including our own, has shown that the epithelial IL-10R1 contributes fundamentally to resistance to intestinal inflammation and represents a component of epithelial innate immunity originally described to be induced by cytokines such as IFN-γ[8]. For instance, mice deficient in IL-10 or IL-10 receptor develop spontaneous severe colitis and mice conditionally lacking intestinal epithelial IL-10R1 show increased susceptibility to colitis [7, 9, 10].

Metabolomic analysis has revealed that gut bacteria impact host immunity through a variety of metabolites, including indole metabolites [11], which originate from the microbial metabolism of tryptophan. Indole-3-propionic acid (IPA) and indole-3-aldehyde (IAld), which are tryptophan metabolites produced by intestinal bacteria, are known for their intercellular signaling activity. Further,

IAld has recently been identified as an aryl hydrocarbon receptor (AHR) ligand [12]. AHR is a ligand-dependent transcription factor activated by a variety of synthetic and biological molecules that plays an important role in immunological response and inhibition of inflammation [13]. AHR contributes to immune homeostasis through various methods, including T cell differentiation and Th17 development [14, 15], as well as the upregulation of IL-22 production [16]. Recently, several studies have shown that the host microbiota provides a consistent source of endogenous AHR ligands with distinct effects on immune homeostasis [16-18]. However, the precise role of indole metabolites in the gastrointestinal tract remains elusive. Together, these data lead us to hypothesize that microbial-derived indole metabolites promote intestinal homeostasis through AHR-mediated regulation of the IEC IL-10R1.

Materials and Methods

Animal Studies

For metabolomics analysis, C57BL/6-129 mice were administered 3% (wt/vol) dextran sodium sulfate (DSS; molecular weight 36,000-50,000; MP Biochemicals, Burlingame, CA) in drinking water for 5 d, followed by a 2-d recovery period. Normal tap water was returned during these 2 d prior to tissue collection. Control mice were maintained on tap water for 7 d. In subsequent animal experiments, 8-12 wk-old C57BL/6 mice were administered water or 2.5% DSS *ad libitum* for 9 d. This administration approach varied slightly to account for a change in death susceptibility to DSS. DSS was then removed and mice were allowed to recover for 2 d prior to euthanasia. For IPA treatment experiments, the addition of IPA at 0.1 mg/ml was administered to water- and DSS-treated animals. Mice were housed in accordance with guidelines from the American Association for Laboratory Animal Care and Research Protocols, and all animal work was approved by the Institutional Animal Care and Use Committee of the University of Colorado. 10mg in 103ml DI H2O

Cell Lines and shRNA Knockdown

Human T84 intestinal epithelial cells (IEC) were cultured in 1:1 DMEM-Ham's F12 with 2.5 mM L-glutamine and 10% FBS. Cells were maintained at 37°C with 5% CO_2. Transepithelial electrical resistances (TEER) were monitored using an EVOM2 Voltohmmeter (World Precision Instruments, Sarasota, FL). Cytokines were purchased from R&D Systems (Minneapolis, MN). IAld, IPA, and AHR inhibitor, CH-223191, were obtained from Sigma Aldrich (St. Louis, MO). 6-formylindole[3,2-b] carbazole (FICZ) was obtained from Tocris Bioscience (Bristol, United Kingdom). All compounds were used at indicated concentrations. Human intestinal organoids (HIOs) were derived following previously described methods [19] and kindly provided by Dr. Jason Spence at the University of Michigan. HIOs were maintained by embedding in Matrigel (BD Biosciences) and applying Advanced DMEM-F12 medium (Invitrogen, Carlsbad, CA) containing 1X B27 supplement (Invitrogen), 1X GlutaMAX (Life Technologies, Carlsbad, CA), 10 μM Hepes, 10% pen/strep, 100 ng/mL rhNoggin (R&D Systems), 100

ng/mL epidermal growth factor (R&D Systems), and approximately 500 ng/mL R-Spondin1 (RSPO1). RSPO1 was obtained from conditioned media collected from a HEK293 cell line that was stably transfected and zeocin-selected for the RSPO1 expression vector. Media was changed every two to four days, and HIOs were transferred to fresh Matrigel once a week until they reached approximately 0.5 mm to 1 mm in size for experiments and RNA isolation. Lentiviral particles encoding shRNA directed against ARNT (MISSION TRC shRNA, University of Colorado Functional Genomics Facility) were used to transduce T84 cells using standard protocols. Stable integration was achieved by puromycin selection at 6 μg/ml. Knockdown was confirmed by qPCR analysis, indicating 80-85% depletion of ARNT levels.

RNA Isolation and Real-Time PCR

Total RNA was extracted from cells using TRIzol (Invitrogen) and from tissue using RNeasy Mini Kit (Qiagen, Hilden Germany). cDNA was prepared using iScript cDNA synthesis kit (Bio-Rad, Hercules, CA). Real-time PCR to measure transcript was carried out in 1× Power SYBR Green master mix (Applied Biosystems, Foster City, CA) using an ABI 7300 thermocycler. Fold change in expression of target mRNA relative to β-actin mRNA was calculated as previously described [20]. Total RNA from HIOs was isolated using Direct-zol RNA Miniprep Kit (Zymo Research Corp, Irvine, CA). Fold change in expression of mRNA transcript from HIO experiments was calculated relative to HSPCB (heat shock protein 90 alpha family class B member 1). Human and mouse primer sequences listed in Table 1.

Western Blot

Whole cell and tissue lysates was extracted in Tris-Lysis buffer on ice and disrupted by sonication. Protein content was quantified using BCA protein assay reagent (Thermo Scientific, Waltham, MA) and 30 μg of whole cell or tissue extract was boiled in Laemmli buffer in reducing conditions subjected to SDS/PAGE. The SDS/PAGE was transferred onto a PVDF membrane and probed for IL-10R1 using a rabbit polyclonal IL-10RA antibody (1: 1000; Thermo Fisher, Waltham, MA) and β-actin (1: 10,000; Abcam, Cambridge, UK).

Metabolomic Analysis

Distal colon tissue (1 cm) was collected from control and DSS-treated mice. Tissues were flash frozen and placed at -80˚C. Global metabolomics was performed by Metabolon, Inc. (Durham, NC). Briefly, tissue samples were thawed and weighed in tared cryovials and 80% ice-cold methanol was added at a ratio of 75µL solvent per mg of sample, then incubated overnight at 4˚C to extract biochemicals. Internal standards were included to control for extraction efficiency. Following methanol extraction, colon samples were processed and analyzed as previously described [21].

HPLC Metabolite Analysis

Indole derivatives were quantified in mouse and human samples using reversed-phase high-performance liquid chromatography with electrochemical coulometric array detection (EC-HPLC; CoulArray, Thermo Scientific, Waltham, MA). Archived human serum samples from patients diagnosed with IBD or from healthy individuals were obtained under research protocols approved by the Colorado Multi-Institutional Review Board. Study participant demographics are listed in Table 2. Tissue and serum samples were extracted in 80% methanol and protein precipitate was removed by centrifugation at 15,000 x *g*. Separation was achieved using an Acclaim Polar Advantage II C18 column (Thermo, Waltham, MA) at a flow rate of 1 ml/min on a gradient of 10% to 55% acetonitrile in 50 mM sodium phosphate buffer, pH 3, containing 0.42 mM octanesulphonic acid as an ion-pairing agent. Calibration curves were composed by performing linear regression analysis of the peak area versus the analyte concentration. The data were quantified using the peak area in comparison to standards.

Bacterial Strains and Gnotobiotic Colonization Experiments

Escherichia coli (*E. coli*) strains were obtained from GE Dharmacon (Lafayette, CO). An *E. coli* K12 parent strain (*E. coli* BW25113; *WT)*, along with strains containing a deletion of *tnaA* (*E. coli JW3686*; Δ*tnaA*) and *tnaB* (*E. coli* JW5619; Δ*tnaB*) were used for experiments. All strains were grown in Lysogeny

broth (LB; 10g/L tryptone, 10g/L NaCl, 5 g/L yeast extract) or on LB-agar plates supplemented with appropriate antibiotics (kanamycin, 50 µg/ml), if needed. Cultures were grown overnight at 37˚C to stationary phase and tested for the presence of indole by the addition of 200 µL of Kovac's reagent (Sigma Aldrich, St. Louis, MO) to 2 mL bacterial culture. For T84 cell experiments, cultures were grown overnight at 37˚C to stationary phase. Briefly, cultures were spun, supernatants collected, and afterward serially diluted and placed onto cells for 24 hr. Bacterial supernatants used for EC-HPLC analysis were placed through a 0.22 µm filter prior to run. For gnotobiotic colonization experiments, 5-8-week-old germ-free C57BL/6 mice were gavaged with a 100 µL bacterial suspension for mono-association (10^9 CFU of each bacterial strain collected from a stationary-phase culture and re-suspended in PBS). Mice were colonized for 2 wk prior to euthanasia. Fresh fecal pellets were collected periodically, weighed, homogenized and serially diluted in PBS for plating to determine bacterial CFU per g of feces.

Histology

Colon samples were fixed in 10% neutral buffered formalin and paraffin embedded prior to staining with hematoxylin and eosin (H&E). All histological quantitation was performed blinded by the same individual using a scoring system previously described [22]. Briefly, the three independent parameters measured were severity of inflammation (0–3: none, slight, moderate, severe), extent of injury (0–3: none, mucosal, mucosal and submucosal, transmural), and crypt damage (0–4: none, basal 1/3 damaged, basal 2/3 damaged, only surface epithelium intact, entire crypt and epithelium lost). The score of each parameter was multiplied by a factor reflecting the percentage of tissue involvement (x1: 0–25%, x2: 26–50%, x3: 51–75%, x4: 76–100%) and all numbers were summed. Maximum possible score was 40.

Quantification of Cytokines in Colon Tissue

For cytokine analysis, colon tissue was extracted in Tris-Lysis buffer by sonication and protein homogenates were quantified using BCA protein assay reagent (Thermo Scientific, Waltham, MA). Tissue concentrations of cytokines were measured using a proinflammatory cytokine screen (Meso Scale

Discovery, Rockville, MD). Assays were performed according to manufacturer's instructions. Cytokine concentrations were normalized to total protein concentration.

Quantification and Statistical Analysis

Data are expressed as mean ± S.E.M. Statistical analyses were performed in GraphPad Prism (La Jolla, CA, Version 7.0) using two-tailed unpaired Student's *t*-test for direct comparisons and one-way or two-way ANOVA with Tukey's test for multiple comparisons. Statistical differences reported as significant when $P < 0.05$.

Results

Tryptophan-indole metabolism is altered in murine and human colitis

To better understand microbe-derived factors that contribute to intestinal homeostasis, we performed a comprehensive, unbiased screen of serum and colonic tissue metabolites from healthy and DSS colitic mice. Mice were administered DSS via drinking water, and serum and colonic tissue were collected during peak disease (day 7). Of the microbe-derived metabolites, most notable were decreases in tryptophan-indole metabolites in both serum and colons of colitic mice compared to mice administered water alone (Figure 1A). Tryptophan is metabolized through various pathways, including the indole pathway, resulting in derivatives that are produced from metabolism by gut microbiota (Figure 1B). Colitis profoundly altered tryptophan metabolism, specifically revealing a selective decrease in indole metabolites. To validate this mass spectrometry-based metabolite screen, we developed an HPLC-based protocol using electrochemical (EC) detection methods (Figure 1C). Eight- to ten-week-old C57BL/6 mice were administered water or 2.5% DSS *ad libitum* for 9 d. DSS was then removed and mice were allowed to recover for 2 d prior to euthanasia. Serum indole metabolites were profiled by EC-HPLC (Figure 1D). Serum indole and IPA levels were significantly decreased in actively colitic animals ($P < 0.05$). A marked decrease in serum IAld was also observed ($P = 0.09$). It is notable that overall tryptophan levels in DSS colitis actually increase (Figure 1A), suggesting that our findings of indole depletion are not a result of diminished tryptophan absorption.

Guided by results of indole depletion in active murine colitis, we attempted to translate our results to human patients. Here, we used our developed EC-HPLC method to quantify various indole metabolites in serum samples from patients with UC. For these purposes, serum samples from healthy controls (n = 20), subjects with active UC (n = 15), and subjects with UC in remission (n = 20) were profiled (see Table 2 for demographics). This analysis revealed that serum IPA was deceased by nearly 60% in subjects with active UC compared to healthy controls ($P < 0.05$, Figure 1E). Notably, this IPA deficiency normalized in UC patients in remission, implicating IPA as both a biomarker for active UC as well as an

indicator of disease remission in human UC. Based on these findings, we further explored the role of indole and metabolites IPA and IAld on intestinal epithelial function.

Indole metabolites induce IL-10R1 expression on intestinal epithelia and improve barrier formation

We have previously shown that tryptophan metabolites are important regulators of IL-10R1 in IEC [23]. Guided by our unbiased metabolomic profile of serum and colon tissue from healthy and DSS-colitic mice and our recent work identifying the epithelial interleukin-10 receptor as the dominant signature for resolution of inflammation in DSS colitis[6, 7], we hypothesized that indole-containing tryptophan metabolites regulate intestinal homeostasis via regulation of epithelial IL-10R1 expression. To examine the induction of IL-10R1 in response to indole metabolites, T84 IEC were exposed to IPA or IAld for 6 h. qPCR of IL-10R1 transcript levels showed a concentration-dependent induction of IL-10R1 (Figure 2A). These findings were not limited to colonic cancer cell lines. Human intestinal organoids (HIOs) are complex three-dimensional spheroid tissues derived from human pluripotent stems cells (hPSCs) [19] and contain the majority of functional epithelial cell types (i.e. enterocytes, goblet, Paneth, enteroendocrine, intestinal stem cells) and structures (i.e. brush borders of microvilli, crypt-like structures, and a mesoderm layer) comprising the human small intestine [24]. HIOs treated with IPA exhibited increasing levels of IL-10R1 transcript, with significant induction at 24 h ($P < 0.001$; Figure 2B). Further analysis revealed a prominent induction of IL-10R1 protein expression in T84 IEC exposed to IPA and IAld (Figure 2C).

We next examined the influence of the metabolite IAld on barrier formation in T84 cell monolayers, as our previous work has demonstrated that IL-10 signaling is important in IEC barrier development and maintenance [7, 23]. Cells exposed to both IAld and IL-10 exhibited significantly increased barrier formation at 72 h compared with untreated cells as measured by TEER ($P < 0.01$; Figure 2D). Further, IAld in combination with IL-10 (10ng/ml) significantly induced Suppressor of Cytokine Signaling 3 (SOCS3), an IL-10-responsive gene that has been found to be protective in intestinal inflammation [25] ($P < 0.05$; Figure 2E). From this perspective, it is notable that SOCS3 was not induced by

IL-10 alone as a result of nearly undetectable levels of IL-10R1 at baseline [6, 7]. Overall, these results identify indole metabolite-dependent induction of the epithelial IL-10R1 as a target pathway for mucosal homeostasis.

Loss of indole-dependent IL-10R1 induction in cells lacking ARNT

We next sought to define the mechanism of indole signaling in intestinal epithelia. Others have shown that tryptophan metabolites function as endogenous ligands for AHR [26]. To determine the relative contribution of AHR to indole signaling, we utilized short hairpin RNA knockdown to deplete the AHR dimeric partner ARNT and examined IL-10R1 induction as an endpoint. Lentiviral shRNA-mediated knockdown of ARNT (shARNT) in T84 IEC resulted in significantly reduced ARNT mRNA expression (81 ± 5% decrease, $P < 0.01$) relative to cells containing a non-template control (shNTC) (Figure 3A). A broader examination of classical AHR-ARNT target genes [26-28] revealed that transcript levels of CYP1A1 and CYP1B1 were significantly increased in shNTC cells treated with IAld compared to untreated shNTC cells. Both targets were also significantly increased in the IAld-treated shNTC compared to shARNT T84 IEC following IAld treatment ($P < 0.01$, $P < 0.05$, respectively; Figure 3B). Analysis of these ARNT-deficient cells revealed a prominent decrease in IAld-dependent induction of IL-10R1 transcript and protein ($P < 0.05$; Figures 3C-E). The AHR small-molecule inhibitor, CH-223191, serves as a specific AHR antagonist. shNTC and shARNT T84 IEC were exposed to IAld (1mM), CH-223191 (10μM), or in combination for 24 h. IAld treatment alone significantly increased IL-10R1 expression at 24 h. CH-223191 significantly reduced IAld-mediated IL-10R1 induction, supporting our hypothesis that IAld modulates IL-10R1 expression via an AHR-mediated mechanism ($P < 0.05$, Figure 3F). These results suggest that the AHR pathway is involved in the indole metabolite-dependent expression of IL-10R1 in IEC.

Bacterial indole production induces IL-10R1

We next sought to determine whether microbe-derived sources of indole could similarly regulate epithelial target genes. For these purposes, we targeted indole production in *Escherichia coli* (*E. coli*). Indole is synthesized from tryptophan by microbial tryptophanase [29]. Using Kovac's reagent to test for the presence of indole, we show that an *E. coli* K12 strain (*E. coli* BW25113; *WT*) clearly produced indole (Figure 4A), whereas deletion of the tryptophanase gene *(*Δ*tnaA)* revealed a lack of detectable indole. Conversely, deletion of one of the tryptophan transporters *(*Δ*tnaB*) does not compromise indole production (Figure 4A). To validate these observations, the presence of indole in cell-free supernatants of bacteria was examined by EC-HPLC. While *E. coli WT* bacteria exhibited readily detectable levels of indole, metabolism of tryptophan to indole was completely abolished in *E. coli* Δ*tnaA* (Figure 4B). To test the activity of this microbial-derived indole, cell-free supernatants from *E. coli WT* and Δ*tnaA* mutant were serially diluted and exposed to T84 IEC for 24 h. Supernatants from *E. coli WT* readily induced IL-10R1 protein expression, while minimal IL-10R1 induction was observed in cells exposed to *E. coli* Δ*tnaA* supernatant (Figure 4C).

We extended these findings to an *in vivo* model. Herein, we examined the function of indole-producing bacteria on epithelial IL-10R1 in germ-free mice. Germ-free mice were colonized with *E. coli WT* or *E. coli* Δ*tnaA* for 2 wk followed by euthanasia. Fresh fecal pellets were collected periodically for plating to ensure equal colonization, quantified as bacterial CFU per g of feces (data not shown). Indole concentrations in cecal contents were validated by HPLC in vehicle and colonized animals. Mice monocolonized with *E. coli WT* displayed significantly increased cecal indole, while negligible levels were measured in PBS- and *E. coli* Δ*tnaA*-gavaged animals ($P < 0.01$; Figure 4D). Further, colons were harvested and RNA extracted for qPCR analysis. This strategy revealed that mice monocolonized with *E. coli WT* displayed significantly increased colonic *il10r1* expression, while no significant *il10r1* induction was observed in colon tissue of mice colonized with *E. coli* Δ*tnaA* mutant ($P < 0.05$; Figure 4E). Taken together, these *in vitro* and *in vivo* results strongly support our hypothesis that microbe-derived indoles promote epithelial homeostasis.

IPA improves DSS colitis outcomes

Given the observation that indole metabolites are significantly decreased in active colitis, we tested the therapeutic potential of IPA in murine colitis outcomes. For these purposes, mice were administered either normal drinking water, DSS (2.5% wt/vol) or a combination of DSS and IPA (0.1 mg/ml) in drinking water for 9 d, followed by DSS removal and a 2-d recovery. To verify that oral administration normalized IPA levels, colonic IPA was quantified by EC-HPLC. This analysis revealed that while DSS colitic mice displayed significantly lower levels of IPA, oral administration of IPA normalized colonic levels of this metabolite ($P < 0.01$; Figure 5A). Under these treatment conditions, DSS/IPA-treated animals displayed significantly less reduction in colon length, a marker of intestinal inflammation, compared to DSS-treated animals ($P < 0.05$; Figure 5B). Histological analysis revealed that DSS/IPA-treated mice displayed attenuated inflammatory infiltration and decreased loss of architecture in comparison to mice treated with DSS alone, which displayed pronounced loss of epithelium and tissue architecture (Figure 5C). These differences resulted in greater histopathological severity scores ($P < 0.001$; Figure 5D). We additionally examined tissue cytokine levels in these mice. Pro-inflammatory cytokine levels were dramatically increased in DSS-treated mice, specifically IFN-γ ($P < 0.05$; Figure 5E), TNF-α ($P < 0.01$; Figure 5F), and IL-1β ($P < 0.05$; Figure 5G), while cytokine levels in DSS/IPA-treated mice were similar to mice administered water alone. Similarly, IL-10 levels were significantly increased in DSS-treated mice, though IPA administration did not alter levels of this cytokine (Supplemental Figure S1). Further, IPA administration increased transcript and protein levels of AHR target genes (Supplemental Figure S2). Taken together, these results indicate that therapeutic normalization of IPA during active colitis attenuates disease and promotes intestinal homeostasis.

Discussion

Recent efforts to define the complex nature of IBD have focused on the contribution of the host microbiota. It is now established that altered microbial composition, termed dysbiosis, is strongly associated with IBD [30] and other intestinal diseases [31]. Such dysbiosis is thought to alter the immune response and influence epithelial function, resulting in increased intestinal permeability [32]. The particular components of the microbiome that promote disease and distinguish phenotypes are not well understood. In the current work, we sought to identify and characterize microbial-derived metabolites that contribute to colonic disease and homeostasis.

Immunometabolism is an area of significant interest in mucosal inflammation [33]. Guided by an unbiased metabolomic profile of serum and colon tissue from healthy and DSS-colitic mice, we identified a significant shift in tissue-associated, microbiota-derived indole derivatives. We show that tryptophan does not decrease in murine colitis. In fact, tryptophan levels significantly increased in colons of colitic mice. Based on these findings, we believe the observed decrease of indole metabolites to be a result of a selective depletion of tryptophan-indole metabolites due to dysbiosis, rather than poor absorption of tryptophan.

Indole is produced from the action of microbial tryptophanase on tryptophan to produce indole, pyruvate, and ammonia via a β-elimination reaction [34]. Microbes that express tryptophanase have the capacity to utilize tryptophan as a source of nitrogen, carbon, and energy [35]. The *tnaA* gene, encoding tryptophanase, is highly conserved among Gram-negative indole-producing species including *Citrobacter*, *Morganella*, *Klebsiella*, *Providencia*, and *Haemophilus influenzae* type b [36]. The presence of *tnaA* is strongly associated with virulence of *H. influenzae* [37]. At present, we do not know the nature of indole deficiencies associated with active inflammation, though our work is consistent with a study demonstrating that bacterial fermentation metabolites are less abundant in patients with IBD compared with healthy controls [38]. Additionally, Wlodarska et al. have recently shown that microbes of IBD patients have a reduced ability to cleave intestinal mucins and metabolize tryptophan [39]. Such a precedent exists for other microbiota-derived metabolites. For example, studies investigating dysbiosis in IBD have

identified lower concentrations of luminal short chain fatty acids (SCFA) and significant depletion of butyrate-producing organisms (e.g., specific *Faecalibacterium* and *Roseburia* genera) with active colonic disease [40-42]. It is therefore likely that our observed decreases in indole metabolism reflect inflammation-associated dysbiosis.

Some evidence exists that microbial-derived indole and indole metabolites could be anti-inflammatory. For instance, Shimada *et. al.* demonstrated that indole administration to germ-free mice increased the expression of some epithelial tight junction proteins and attenuated weight loss in a DSS colitis model [43]. No mechanisms were evaluated to describe these changes elicited by indole. Moreover, Venkatesh et al. have shown that IPA is a ligand for the pregnane X receptor (PXR) and promotes intestinal barrier integrity through down-regulation of epithelial TNFα, induction of MDR1, and regulation of epithelial junctional complexes [44]. It is interesting to note that PXR, a member of the superfamily of nuclear receptors, is under consideration as a novel drug target in IBD [45]. Further, Wlodarska et al. have shown that the metabolite indoleacrylic acid promotes intestinal barrier function and mitigates inflammatory responses through downregulation of genes involved in inflammation and oxidative stress [39]. Conversely, it is also notable that some indole derivatives have also been shown to be nephrotoxic. For example, Devlin et al. recently identified a widely distributed family of tryptophanases produced by commensal *Bacteroides* within in the gut microbiota [46]. They demonstrate that microbe-derived indoles are modified by the host to generate toxic renal levels of indoxyl sulfate and that colonization with tryptophanase-deficient *Bacteroides* decreases systemic levels of indoxyl sulfate that may be renal protective.

We translated these findings of shifts in indole metabolism from murine colitis to human subjects. This analysis revealed, for the first time, that serum indole metabolites in human subjects with active UC revealed a remarkable similarity to mice with active colitis, with the exception that human subjects were selectively deficient in IPA and not indole or IAld. The reason for this selective loss of IPA in humans is not known. It should be noted that indole and indole metabolites are produced by different pathways and different bacteria. Since IPA is an indole derivative conjugated to propionate and propionate is among the

SCFAs that become depleted in active human IBD [47], it is possible that this selective depletion of IPA is explained by an IBD-associated dysbiosis that results from the combined depletion of both SCFA- and indole-producing microbiota. Further studies will be necessary to define the nature of this observation.

Therapeutic administration of oral IPA was protective in a murine model of colitis. Animals that received IPA not only exhibited fewer physical signs of disease, but also had significantly less damage to crypt structure and restricted inflammatory infiltration. Indoles and other tryptophan metabolites have been demonstrated to function as AHR ligands [26, 48, 49]. It is likely that as AHR ligands, these molecules directly influence the epithelial/immune cell axis. For example, Zelante et al. showed that IAld drives AHR-dependent IL-22 production and mucosal protection. Others have shown that innate lymphoid cell AHR responses to be protective in inflammation through the production of IL-22 [16]. It is also noteworthy that intraepithelial lymphocytes localize in response to AHR stimulation by dietary ligands [50], including specific $CD4^+CD8\alpha\alpha^+$ subsets of intraepithelial T cells [51]. The activity of AHR ligands on intestinal epithelia is less well understood. Similar to indole metabolites, we recently demonstrated that other tryptophan-derived metabolites, including kynurenine, regulate epithelial IL-10R1 activity in an AHR-dependent manner [23]. Such activity was associated with protection in colitis models and promoted epithelial wound healing. These varied ligands suggest a promiscuous ligand-binding pocket of AHR that is associated with agonistic activity [52]. Moreover, these results suggest redundant mechanisms to maintain expression of functional epithelial IL-10 receptors, which have been shown to be essential for the development and maintenance of barrier function [7].

Finally, it is known that colitis occurs as the result of immune cell responses to microbiota in susceptible hosts [53]. These interactions are complex, involving multiple cell types and a spectrum of metabolites. In this regard, we cannot rule out the contribution of cell types beyond the epithelium (e.g. immune cells) in regulation by bacterial-derived metabolites in DSS. Rather, it is likely that these metabolites have a plethora of actions on various cell types in the mucosa. In our studies, we have limited this analysis to the epithelium to allow for a deeper and more mechanistic understanding of these signaling responses. These studies provide strong evidence for the role of microbiota-derived indole

metabolites in anti-inflammatory pathways mediated by IL-10 signaling in the intestinal epithelium. These findings present new insight to our understanding of host-microbial communication within the mucosa and identify possible avenues for utilizing indoles as novel therapeutics in mucosal disease.

Acknowledgements

EEA, DJK, and SPC designed the study. EEA, JML, DJK, ELC, CJK, and KDB performed experiments. MEG provided human serum samples. BRJ, STW, and DJK provided germ free mice, human intestinal organoids and corresponding *in vitro* experiments. EEA and SPC wrote the manuscript, all authors read and edited the manuscript. Thank you to Dr. Jason Spence and Sha Huang (University of Michigan) for developing the human intestinal organoids from human pluripotent stem cells.

References

[1] Lozupone CA, Stombaugh JI, Gordon JI, Jansson JK, Knight R: Diversity, stability and resilience of the human gut microbiota. Nature 2012, 489:220-30.

[2] Muniz LR, Knosp C, Yeretssian G: Intestinal antimicrobial peptides during homeostasis, infection, and disease. Frontiers in immunology 2012, 3:310.

[3] Xavier RJ, Podolsky DK: Unravelling the pathogenesis of inflammatory bowel disease. Nature 2007, 448:427-34.

[4] Huttenhower C, Kostic AD, Xavier RJ: Inflammatory bowel disease as a model for translating the microbiome. Immunity 2014, 40:843-54.

[5] Frank DN, St Amand AL, Feldman RA, Boedeker EC, Harpaz N, Pace NR: Molecular-phylogenetic characterization of microbial community imbalances in human inflammatory bowel diseases. Proc Natl Acad Sci U S A 2007, 104:13780-5.

[6] Engelhardt KR, Grimbacher B: IL-10 in humans: lessons from the gut, IL-10/IL-10 receptor deficiencies, and IL-10 polymorphisms. Current topics in microbiology and immunology 2014, 380:1-18.

[7] Kominsky DJ, Campbell EL, Ehrentraut SF, Wilson KE, Kelly CJ, Glover LE, Collins CB, Bayless AJ, Saeedi B, Dobrinskikh E, Bowers BE, MacManus CF, Muller W, Colgan SP, Bruder D: IFN-gamma-mediated induction of an apical IL-10 receptor on polarized intestinal epithelia. J Immunol 2014, 192:1267-76.

[8] Colgan SP, Parkos CA, Matthews JB, D'Andrea L, Awtrey CS, Lichtman A, Delp C, Madara JL: Interferon-γ induces a surface phenotype switch in intestinal epithelia: Downregulation of ion transport and upregulation of immune accessory ligands. Am J Physiol 1994, 267:C402-C10.

[9] Kuhn R, Lohler J, Rennick D, Rajewsky K, Muller W: Interleukin-10-deficient mice develop chronic enterocolitis. Cell 1993, 75:263-74.

[10] Chaudhry A, Samstein RM, Treuting P, Liang Y, Pils MC, Heinrich JM, Jack RS, Wunderlich FT, Bruning JC, Muller W, Rudensky AY: Interleukin-10 signaling in regulatory T cells is required for suppression of Th17 cell-mediated inflammation. Immunity 2011, 34:566-78.

[11] Wikoff WR, Anfora AT, Liu J, Schultz PG, Lesley SA, Peters EC, Siuzdak G: Metabolomics analysis reveals large effects of gut microflora on mammalian blood metabolites. Proc Natl Acad Sci U S A 2009, 106:3698-703.

[12] Zelante T, Iannitti RG, Cunha C, De Luca A, Giovannini G, Pieraccini G, Zecchi R, D'Angelo C, Massi-Benedetti C, Fallarino F, Carvalho A, Puccetti P, Romani L: Tryptophan catabolites from microbiota engage aryl hydrocarbon receptor and balance mucosal reactivity via interleukin-22. Immunity 2013, 39:372-85.

[13] Hubbard TD, Murray IA, Bisson WH, Lahoti TS, Gowda K, Amin SG, Patterson AD, Perdew GH: Adaptation of the human aryl hydrocarbon receptor to sense microbiota-derived indoles. Scientific reports 2015, 5:12689.

[14] Mascanfroni ID, Takenaka MC, Yeste A, Patel B, Wu Y, Kenison JE, Siddiqui S, Basso AS, Otterbein LE, Pardoll DM, Pan F, Priel A, Clish CB, Robson SC, Quintana FJ: Metabolic control of type 1 regulatory T cell differentiation by AHR and HIF1-alpha. Nature medicine 2015, 21:638-46.

[15] Kimura A, Naka T, Nohara K, Fujii-Kuriyama Y, Kishimoto T: Aryl hydrocarbon receptor regulates Stat1 activation and participates in the development of Th17 cells. Proceedings of the National Academy of Sciences of the United States of America 2008, 105:9721-6.

[16] Monteleone I, Rizzo A, Sarra M, Sica G, Sileri P, Biancone L, MacDonald TT, Pallone F, Monteleone G: Aryl hydrocarbon receptor-induced signals up-regulate IL-22 production and inhibit inflammation in the gastrointestinal tract. Gastroenterology 2011, 141:237-48, 48 e1.

[17] Gaitanis G, Magiatis P, Stathopoulou K, Bassukas ID, Alexopoulos EC, Velegraki A, Skaltsounis AL: AhR ligands, malassezin, and indolo[3,2-b]carbazole are selectively produced by Malassezia furfur strains isolated from seborrheic dermatitis. The Journal of investigative dermatology 2008, 128:1620-5.

[18] Vlachos C, Schulte BM, Magiatis P, Adema GJ, Gaitanis G: Malassezia-derived indoles activate the aryl hydrocarbon receptor and inhibit Toll-like receptor-induced maturation in monocyte-derived dendritic cells. The British journal of dermatology 2012, 167:496-505.

[19] McCracken KW, Howell JC, Wells JM, Spence JR: Generating human intestinal tissue from pluripotent stem cells in vitro. Nat Protoc 2011, 6:1920-8.

[20] Pfaffl MW: A new mathematical model for relative quantification in real-time RT-PCR. Nucleic acids research 2001, 29:e45.

[21] Albrecht E, Waldenberger M, Krumsiek J, Evans AM, Jeratsch U, Breier M, Adamski J, Koenig W, Zeilinger S, Fuchs C, Klopp N, Theis FJ, Wichmann HE, Suhre K, Illig T, Strauch K, Peters A, Gieger C, Kastenmuller G, Doering A, Meisinger C: Metabolite profiling reveals new insights into the regulation of serum urate in humans. Metabolomics : Official journal of the Metabolomic Society 2014, 10:141-51.

[22] Dieleman LA, Palmen MJ, Akol H, Bloemena E, Pena AS, Meuwissen SG, Van Rees EP: Chronic experimental colitis induced by dextran sulphate sodium (DSS) is characterized by Th1 and Th2 cytokines. Clin Exp Immunol 1998, 114:385-91.

[23] Lanis JM, Alexeev EE, Curtis VF, Kitzenberg DA, Kao DJ, Battista KD, Gerich ME, Glover LE, Kominsky DJ, Colgan SP: Tryptophan metabolite activation of the aryl hydrocarbon receptor regulates IL-10 receptor expression on intestinal epithelia. Mucosal Immunol 2017.

[24] Spence JR, Mayhew CN, Rankin SA, Kuhar MF, Vallance JE, Tolle K, Hoskins EE, Kalinichenko VV, Wells SI, Zorn AM, Shroyer NF, Wells JM: Directed differentiation of human pluripotent stem cells into intestinal tissue in vitro. Nature 2011, 470:105-9.

[25] Suzuki A, Hanada T, Mitsuyama K, Yoshida T, Kamizono S, Hoshino T, Kubo M, Yamashita A, Okabe M, Takeda K, Akira S, Matsumoto S, Toyonaga A, Sata M, Yoshimura A: CIS3/SOCS3/SSI3 plays a negative regulatory role in STAT3 activation and intestinal inflammation. J Exp Med 2001, 193:471-81.

[26] Hubbard TD, Murray IA, Perdew GH: Indole and Tryptophan Metabolism: Endogenous and Dietary Routes to Ah Receptor Activation. Drug Metab Dispos 2015, 43:1522-35.

[27] Lo R, Matthews J: High-resolution genome-wide mapping of AHR and ARNT binding sites by ChIP-Seq. Toxicol Sci 2012, 130:349-61.

[28] Mathieu MC, Lapierre I, Brault K, Raymond M: Aromatic hydrocarbon receptor (AhR).AhR nuclear translocator- and p53-mediated induction of the murine multidrug resistance mdr1 gene by 3-methylcholanthrene and benzo(a)pyrene in hepatoma cells. J Biol Chem 2001, 276:4819-27.

[29] Lee JH, Wood TK, Lee J: Roles of indole as an interspecies and interkingdom signaling molecule. Trends Microbiol 2015, 23:707-18.

[30] Manichanh C, Borruel N, Casellas F, Guarner F: The gut microbiota in IBD. Nat Rev Gastroenterol Hepatol 2012, 9:599-608. .

[31] Butto LF, Haller D: Dysbiosis in intestinal inflammation: Cause or consequence. Int J Med Microbiol 2016, 306:302-9. .

[32] Sartor RB: Microbial influences in inflammatory bowel diseases. Gastroenterology 2008, 134:577-94.

[33] Kominsky DJ, Keely S, MacManus CF, Glover LE, Scully M, Collins CB, Bowers BE, Campbell EL, Colgan SP: An endogenously anti-inflammatory role for methylation in mucosal inflammation identified through metabolite profiling. Journal of immunology (Baltimore, Md : 1950) 2011, 186:6505-14.

[34] Newton WA, Snell EE: Catalytic Properties of Tryptophanase, a Multifunctional Pyridoxal Phosphate Enzyme. Proc Natl Acad Sci U S A 1964, 51:382-9.

[35] Hopkins FG, Cole SW: A contribution to the chemistry of proteids: Part II. The constitution of tryptophane, and the action of bacteria upon it. J Physiol 1903, 29:451-66.

[36] Lee JH, Lee J: Indole as an intercellular signal in microbial communities. FEMS Microbiol Rev 2010, 34:426-44. .

[37] Martin K, Morlin G, Smith A, Nordyke A, Eisenstark A, Golomb M: The tryptophanase gene cluster of Haemophilus influenzae type b: evidence for horizontal gene transfer. J Bacteriol 1998, 180:107-18.

[38] De Preter V, Machiels K, Joossens M, Arijs I, Matthys C, Vermeire S, Rutgeerts P, Verbeke K: Faecal metabolite profiling identifies medium-chain fatty acids as discriminating compounds in IBD. Gut 2015, 64:447-+.

[39] Wlodarska M, Luo C, Kolde R, d'Hennezel E, Annand JW, Heim CE, Krastel P, Schmitt EK, Omar AS, Creasey EA, Garner AL, Mohammadi S, O'Connell DJ, Abubucker S, Arthur TD, Franzosa EA, Huttenhower C, Murphy LO, Haiser HJ, Vlamakis H, Porter JA, Xavier RJ: Indoleacrylic Acid Produced by Commensal Peptostreptococcus Species Suppresses Inflammation. Cell Host Microbe 2017, 22:25-37 e6.

[40] Machiels K, Joossens M, Sabino J, De Preter V, Arijs I, Eeckhaut V, Ballet V, Claes K, Van Immerseel F, Verbeke K, Ferrante M, Verhaegen J, Rutgeerts P, Vermeire S: A decrease of the butyrate-producing species Roseburia hominis and Faecalibacterium prausnitzii defines dysbiosis in patients with ulcerative colitis. Gut 2013.

[41] Eeckhaut V, Machiels K, Perrier C, Romero C, Maes S, Flahou B, Steppe M, Haesebrouck F, Sas B, Ducatelle R, Vermeire S, Van Immerseel F: Butyricicoccus pullicaecorum in inflammatory bowel disease. Gut 2013, 62:1745-52.

[42] Sokol H, Seksik P, Furet JP, Firmesse O, Nion-Larmurier I, Beaugerie L, Cosnes J, Corthier G, Marteau P, Dore J: Low counts of Faecalibacterium prausnitzii in colitis microbiota. Inflammatory bowel diseases 2009, 15:1183-9.

[43] Shimada Y, Kinoshita M, Harada K, Mizutani M, Masahata K, Kayama H, Takeda K: Commensal bacteria-dependent indole production enhances epithelial barrier function in the colon. PLoS One 2013, 8:e80604. .

[44] Venkatesh M, Mukherjee S, Wang H, Li H, Sun K, Benechet AP, Qiu Z, Maher L, Redinbo MR, Phillips RS, Fleet JC, Kortagere S, Mukherjee P, Fasano A, Le Ven J, Nicholson JK, Dumas ME, Khanna KM, Mani S: Symbiotic bacterial metabolites regulate gastrointestinal barrier function via the xenobiotic sensor PXR and Toll-like receptor 4. Immunity 2014, 41:296-310. .

[45] Cheng J, Shah YM, Gonzalez FJ: Pregnane X receptor as a target for treatment of inflammatory bowel disorders. Trends Pharmacol Sci 2012, 33:323-30. .

[46] Devlin AS, Marcobal A, Dodd D, Nayfach S, Plummer N, Meyer T, Pollard KS, Sonnenburg JL, Fischbach MA: Modulation of a Circulating Uremic Solute via Rational Genetic Manipulation of the Gut Microbiota. Cell Host Microbe 2016, 20:709-15.

[47] Machiels K, Joossens M, Sabino J, De Preter V, Arijs I, Eeckhaut V, Ballet V, Claes K, Van Immerseel F, Verbeke K, Ferrante M, Verhaegen J, Rutgeerts P, Vermeire S: A decrease of the butyrate-producing species Roseburia hominis and Faecalibacterium prausnitzii defines dysbiosis in patients with ulcerative colitis. Gut 2013, 10:2013-304833.

[48] Heath-Pagliuso S, Rogers WJ, Tullis K, Seidel SD, Cenijn PH, Brouwer A, Denison MS: Activation of the Ah receptor by tryptophan and tryptophan metabolites. Biochemistry 1998, 37:11508-15.

[49] Jin UH, Lee SO, Sridharan G, Lee K, Davidson LA, Jayaraman A, Chapkin RS, Alaniz R, Safe S: Microbiome-Derived Tryptophan Metabolites and Their Aryl Hydrocarbon Receptor-Dependent Agonist and Antagonist Activities. Molecular Pharmacology 2014, 85:777-88.

[50] Li Y, Innocentin S, Withers DR, Roberts NA, Gallagher AR, Grigorieva EF, Wilhelm C, Veldhoen M: Exogenous stimuli maintain intraepithelial lymphocytes via aryl hydrocarbon receptor activation. Cell 2011, 147:629-40.

[51] Cervantes-Barragan L, Chai JN, Tianero MD, Di Luccia B, Ahern PP, Merriman J, Cortez VS, Caparon MG, Donia MS, Gilfillan S, Cella M, Gordon JI, Hsieh CS, Colonna M: Lactobacillus reuteri induces gut intraepithelial CD4+CD8alphaalpha+ T cells. Science 2017, 357:806-10. .

[52] Bessede A, Gargaro M, Pallotta MT, Matino D, Servillo G, Brunacci C, Bicciato S, Mazza EM, Macchiarulo A, Vacca C, Iannitti R, Tissi L, Volpi C, Belladonna ML, Orabona C, Bianchi R, Lanz TV, Platten M, Della Fazia MA, Piobbico D, Zelante T, Funakoshi H, Nakamura T, Gilot D, Denison MS, Guillemin GJ, DuHadaway JB, Prendergast GC, Metz R, Geffard M, Boon L, Pirro M, Iorio A, Veyret B, Romani L, Grohmann U, Fallarino F, Puccetti P: Aryl hydrocarbon receptor control of a disease tolerance defence pathway. Nature 2014, 511:184-90.

[53] Belkaid Y, Hand TW: Role of the microbiota in immunity and inflammation. Cell 2014, 157:121-41.

Figures Legends

Figure 1. Tryptophan metabolism is altered in murine and human colitis. (A) Relative levels of indole metabolites in serum and whole colon tissue of mice receiving either water or 3% DSS for 7 d. Metabolites were measured by LC/MS and GC/MS analysis, n = 5 mice per treatment group. **(B)** Condensed pathway of tryptophan metabolism to indole and indole derivatives. **(C)** EC-HPLC analysis of indole metabolites in serum of mice receiving either water or 2.5% DSS for 9 d. **(D)** Concentrations of indole metabolites in serum of mice receiving either water or 2.5% DSS for 9 d (H2O, n = 5; DSS, n = 10 mice). **(E)** Indole-3-propionic acid (IPA) levels in serum samples from healthy controls (Con; n = 20), subjects with active ulcerative colitis (UC; n = 15) and subjects with UC in remission (Rem; n = 20) profiled by EC-HPLC. Data presented as mean ± S.E.M. **P* < 0.05, ***P* < 0.01, Student's *t*-test and one-way ANOVA.

Figure 2. Indole metabolites improve barrier formation and induce IL-10R1 on intestinal epithelia. **(A)** qPCR of IL-10R1 transcript levels in T84 cells treated with IPA or IAld at varying concentrations for 6 h. **(B)** HIOs treated with 1mM IPA over 24 h. **(C)** Western blot analysis of IL-10R1 levels in T84 cells treated with IPA at varying concentrations for 6 h (+ ctrl: FICZ at 1 μM) or in response to 1 mM IAld over 24 h. **(D)** Transepithelial electrical resistance (TEER) of T84 cells treated with IAld (1 μM), IL-10 (10 ng/ml), or a combination of both was measured over 72 h. Data shown are represented as the average TEER ± S.E.M. of triplicate samples. ***P* < 0.01, compared to untreated cells, two-way ANOVA. **(E)** qPCR of SOCS3 transcript in T84 cells treated with IAld for 12 h, followed by treatment with IL-10 for 6 h. Data are presented as mean ± S.E.M. of at least three independent experiments. **P* < 0.05, ****P* < 0.001, Student's t-test.

Figure 3. IL-10R1 expression is not induced by cells lacking AHR binding partner ARNT. **(A)** Lentiviral shRNA-mediated knockdown of ARNT (shARNT) in T84 intestinal epithelial cells relative to T84 cells containing a non-template control (shNTC). **(B)** Transcript levels of CYP1A1 and CYP1B1

by qPCR in shNTC and shARNT T84 cells following IAld treatment for 12 h. **(C)** qPCR analysis of IL-10R1 expression in shNTC and shARNT T84 cells treated with 1 mM IAld for 24 h. **(D)** Western blot analysis of IL-10R1 levels in ARNT knockdown T84 cells. Confluent monolayers of T84 cells were treated with IAld for 24 h. Protein expression was quantified by densitometry **(E)** and normalized to β-actin. **(F)** qPCR of IL-10R1 transcript levels in shNTC and shARNT T84 cells treated with AHR inhibitor (AHRi, 10 μM), IAld (1 mM), or both for 24 h. Data is presented as mean ± S.E.M. of three independent experiments. *$P < 0.05$, **$P < 0.01$, compared to untreated shNTC, Student's t-test.

Figure 4. Bacterial indole production induces IL-10R1. (A) Indole production test of cultures from *E. coli* K12 wild-type (*WT*), *tnaA* and *tnaB* mutants; "+" indicates presence of indole. **(B)** EC-HPLC chromatogram of supernatants collected from *E. coli* K12 *WT* and *E. coli* Δ*tnaA*. **(C)** T84 cells were treated for 24 h with serially diluted supernatants from *E. coli WT or E. coli* Δ*tnaA* cultures grown to stationary phase, followed by media replenishment (M: molecular marker; + ctrl: IFN-γ at 10 ng/ml). Germ free mice were colonized with *E. coli WT* or *E. coli* Δ*tnaA* for 2 wk followed by euthanasia. **(D)** Indole concentrations in cecal contents were validated by HPLC in vehicle and colonized mice, and **(E)** RNA was extracted from colons for qPCR analysis of Il10r1 expression (PBS, n = 5; *E. coli WT*, n = 4; *E. coli* Δ*tnaA*, n = 5). Data are presented as mean ± S.E.M. *$P < 0.05$, **$P < 0.01$, Student's t-test.

Figure 5. IPA improves DSS colitis outcomes. Eight- to ten-wk-old C57BL/6 mice were administered water or 2.5% DSS ± IPA *ad libitum* for 9 d. DSS was then removed and mice were allowed to recover for 2 d as predetermined prior to euthanasia. **(A)** Concentration of IPA in colons of mice receiving DSS ± IPA for up to 9 d. **(B)** Colon length measured at time of euthanasia. **(C)** Representative H&E-stained colonic sections isolated from H2O-treated, H_2O/IPA-treated, DSS-treated, and DSS/IPA-treated mice at 20X magnification. **(D)** Histologic score of H&E-colonic sections. Colon tissue was homogenized and cytokines were measured in protein lysates by Mesoscale analysis [**(E)** IFN-γ; **(F)** TNF-α; and **(G)** IL-

1β]. Data are presented as mean ± S.E.M. *$P < 0.05$, **$P < 0.01$, ***$P < 0.001$, two-way ANOVA and Student's t-test.

Supplemental Figure S1. IPA upregulates IL-10R1 in DSS colitis. Eight- to ten-wk-old C57BL/6 mice were administered water or 2.5% DSS ± IPA *ad libitum* for 9 d. DSS was then removed and mice were allowed to recover for 2 d as predetermined prior to euthanasia. **(A)** qPCR of Il10r1 transcript levels in colon tissue. **(B)** IL-10 levels in colon tissue protein lysates were measured by Mesoscale analysis. n = 5-10 mice/group. Data are presented as mean ± S.E.M. *$P < 0.05$

Supplemental Figure S2. IPA induces AHR target genes *in vivo.* Transcript levels of **(A)** Cyp1a1 and **(B)** Cyp1b1 were measured in colon tissue of eight- to ten-wk-old C57BL/6 mice administered water or 2.5% DSS ± IPA *ad libitum* for 9 d. **(C)** Further, colon tissue levels of IL-6 were measured in protein lysates by Mesoscale analysis. n = 5-10 mice/group. Data are presented as mean ± S.E.M. *$P < 0.05$

Tables

Table 1. Primer sequences for qPCR.

Gene	Forward Primer	Reverse Primer
hACTB	5'-CCTGGCACCCAGCACAAT-3'	5'-GCCGATCCACACGGAGTACT-3'
hHSPCB	5'-TCTGGGTATCGGAAAGCAAGCC-3'	5'-GTGCACTTCCTCAGGCATCTTG-3'
hIL10R1	5'-CACATCCTCCACTGGACACC-3'	5'-CAAGGTCACTGCGGTAAGGT-3'
hSOCS3	5'-GGCCACTCTTCAGCATCTC-3'	5'-ATCGTACTGGTCCAGGAACTC-3'
hCYP1A1	5'-ACCCGCCACCCTTCGACAGTTC-3'	5'-TGCCCAGGCGTTGCGTGAGAAG-3'
hCYP1B1	5'-CTGGCACTGACGACGCCAAGA-3'	5'-TGGTCTGCTGGATGGACAGC-3'
hMDR1	5'-AACGGAAGCCAGAACATTCC-3'	5'-AGGCTTCCTGTGGCAAAGAG-3'
mActb	5'-TACGGATGTCAACGTCACAC-3'	5'-AAGAGCTATGAGCTGCCTGA-3'
mIl10r1	5'-CCCATTCCTCGTCACGATCTC-3'	5'-TCAGACTGGTTTGGGATAGGTTT-3'

719 **Table 2.** Study participant demographics.

Characteristic	Control	UC Remission	Ulcerative Colitis
Number	20	20	15
Sex			
Male	11	12	13
Female	9	8	2
Age	58.6 ± 10.9	46.5 ± 18.6	40.4 ± 13.4
Disease Location			
Left-sided	n/a	6	1
Extensive	n/a	14	12
Proctitis	n/a	0	2

720

721

722

723

724

725

726

727

728

729

730

731

732

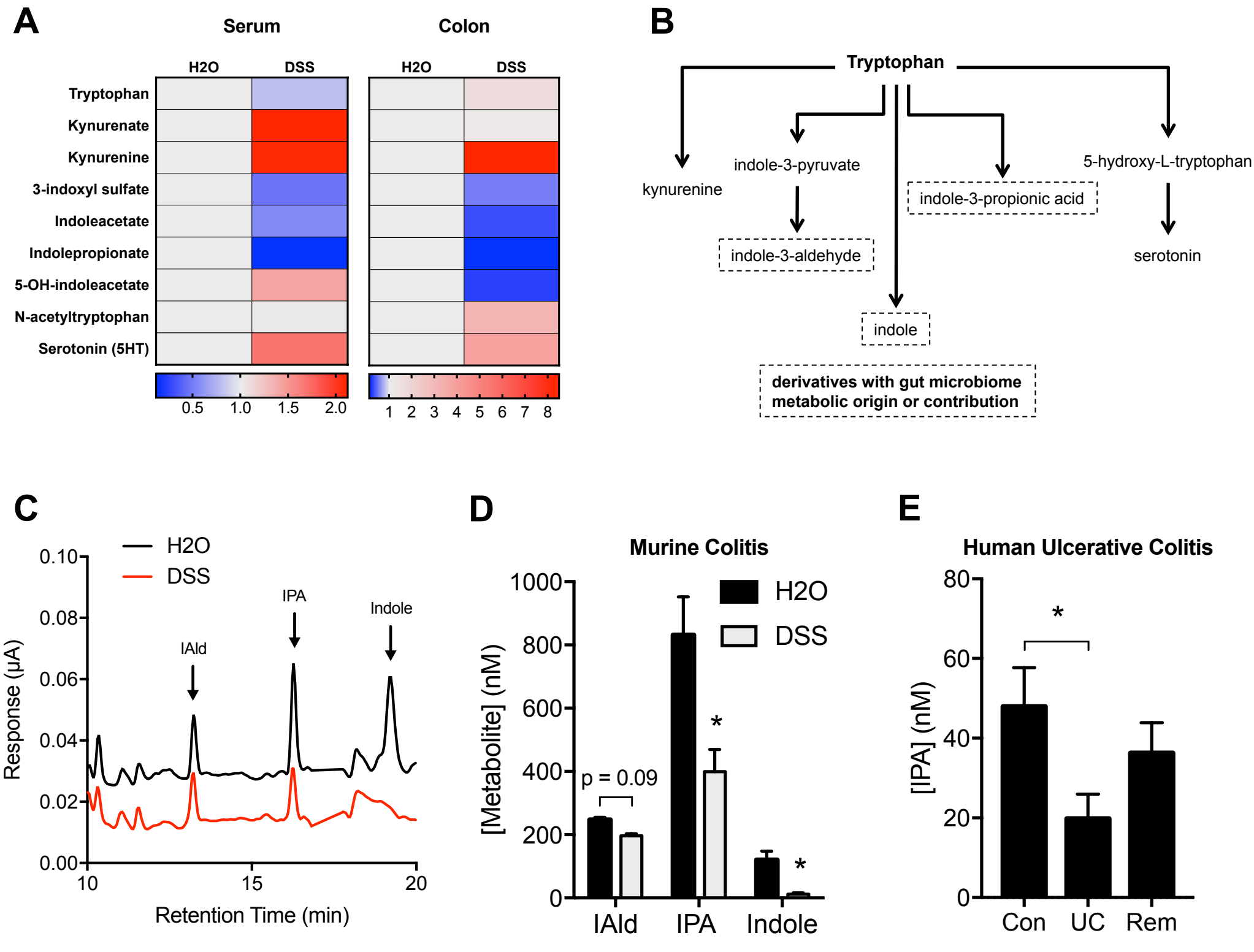
A
Serum
Colon
H2O
DSS
H2O
DSS
Tryptophan
Kynurenate
Kynurenine
3-indoxyl sulfate
Indoleacetate
Indolepropionate
5-OH-indoleacetate
N-acetyltryptophan
Serotonin (5HT)
0.5 1.0 1.5 2.0
1 2 3 4 5 6 7 8
B
Tryptophan
kynurenine
indole-3-pyruvate
indole-3-propionic acid
5-hydroxy-L-tryptophan
indole-3-aldehyde
serotonin
indole
derivatives with gut microbiome metabolic origin or contribution
C
H2O
DSS
IAld
IPA
Indole
Response (μA)
0.10
0.08
0.06
0.04
0.02
0.00
10
15
20
Retention Time (min)
D
Murine Colitis
H2O
DSS
[Metabolite] (nM)
1000
800
600
400
200
0
p = 0.09
*
*
IAld
IPA
Indole
E
Human Ulcerative Colitis
[IPA] (nM)
80
60
40
20
0
*
Con
UC
Rem

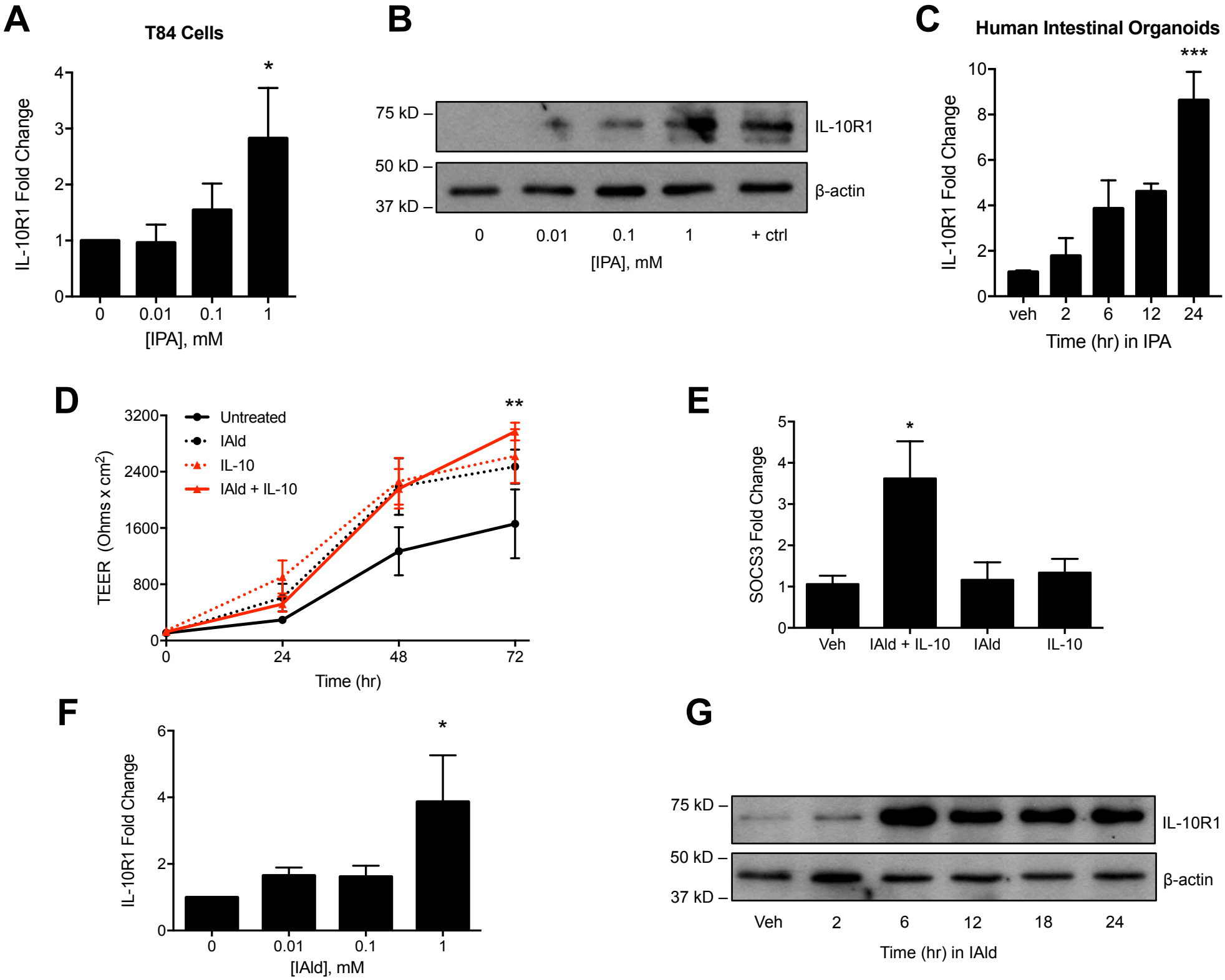
A
T84 Cells
IL-10R1 Fold Change
[IPA], mM
B
75 kD –
50 kD –
37 kD –
IL-10R1
β-actin
0
0.01
0.1
1
+ ctrl
[IPA], mM
C
Human Intestinal Organoids
IL-10R1 Fold Change
***
veh
2
6
12
24
Time (hr) in IPA
D
TEER (Ohms x cm2)
Untreated
IAld
IL-10
IAld + IL-10
**
Time (hr)
E
SOCS3 Fold Change
*
Veh
IAld + IL-10
IAld
IL-10
F
IL-10R1 Fold Change
*
[IAld], mM
G
75 kD –
50 kD –
37 kD –
IL-10R1
β-actin
Veh
2
6
12
18
24
Time (hr) in IAld

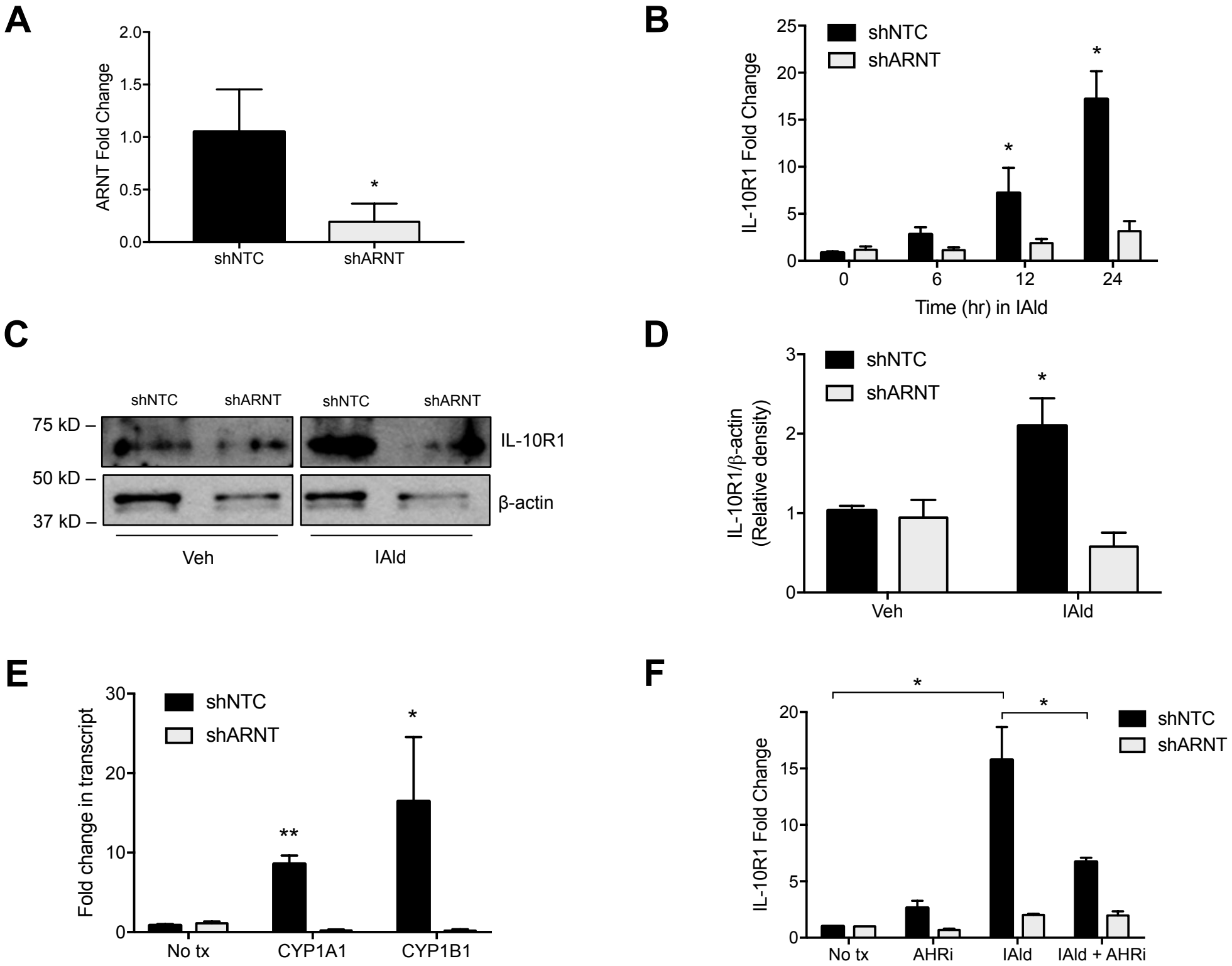
A
ARNT Fold Change
2.0
1.5
1.0
0.5
0.0
*
shNTC
shARNT
B
IL-10R1 Fold Change
25
20
15
10
5
0
shNTC
shARNT
*
*
0
6
12
24
Time (hr) in IAld
C
shNTC
shARNT
shNTC
shARNT
75 kD –
50 kD –
37 kD –
IL-10R1
β-actin
Veh
IAld
D
IL-10R1/β-actin
(Relative density)
3
2
1
0
shNTC
shARNT
*
Veh
IAld
E
Fold change in transcript
30
20
10
0
shNTC
shARNT
**
*
No tx
CYP1A1
CYP1B1
F
IL-10R1 Fold Change
20
15
10
5
0
*
*
shNTC
shARNT
No tx
AHRi
IAld
IAld + AHRi

A

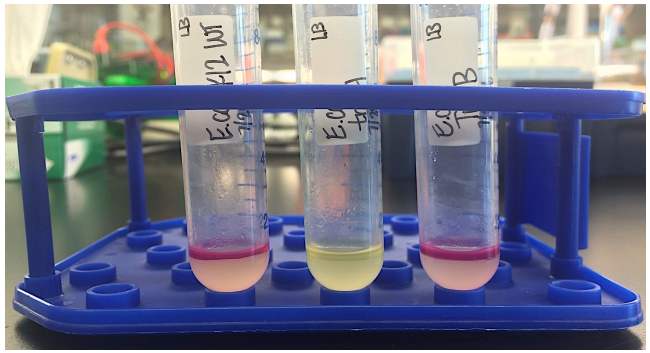

Strain:	*E. coli*^{WT}	*E. coli*$^{\Delta tnaA}$	*E. coli*$^{\Delta tnaB}$
Indole:	+	-	+

B

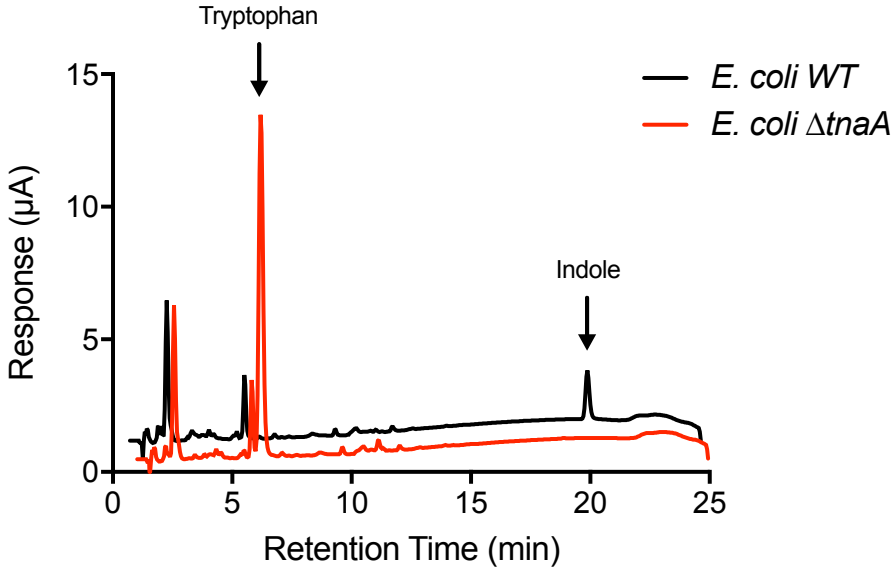

C

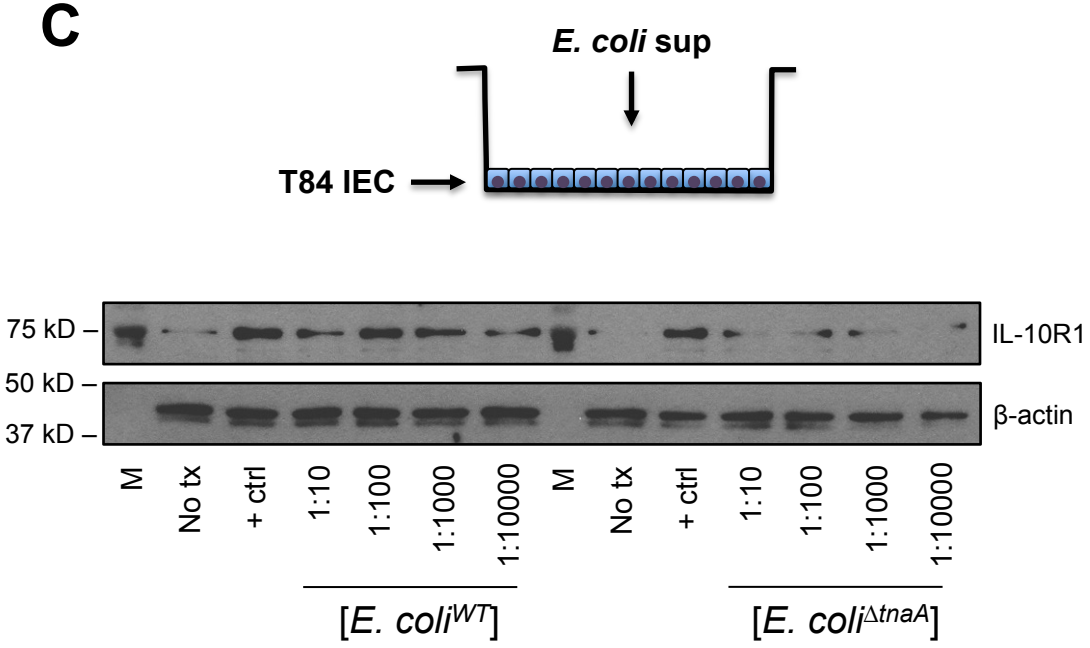

D

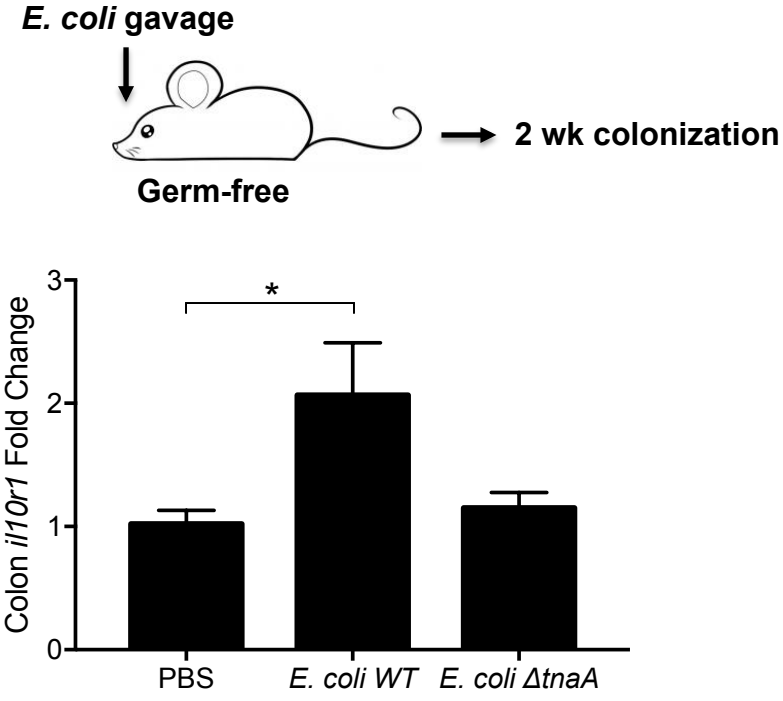

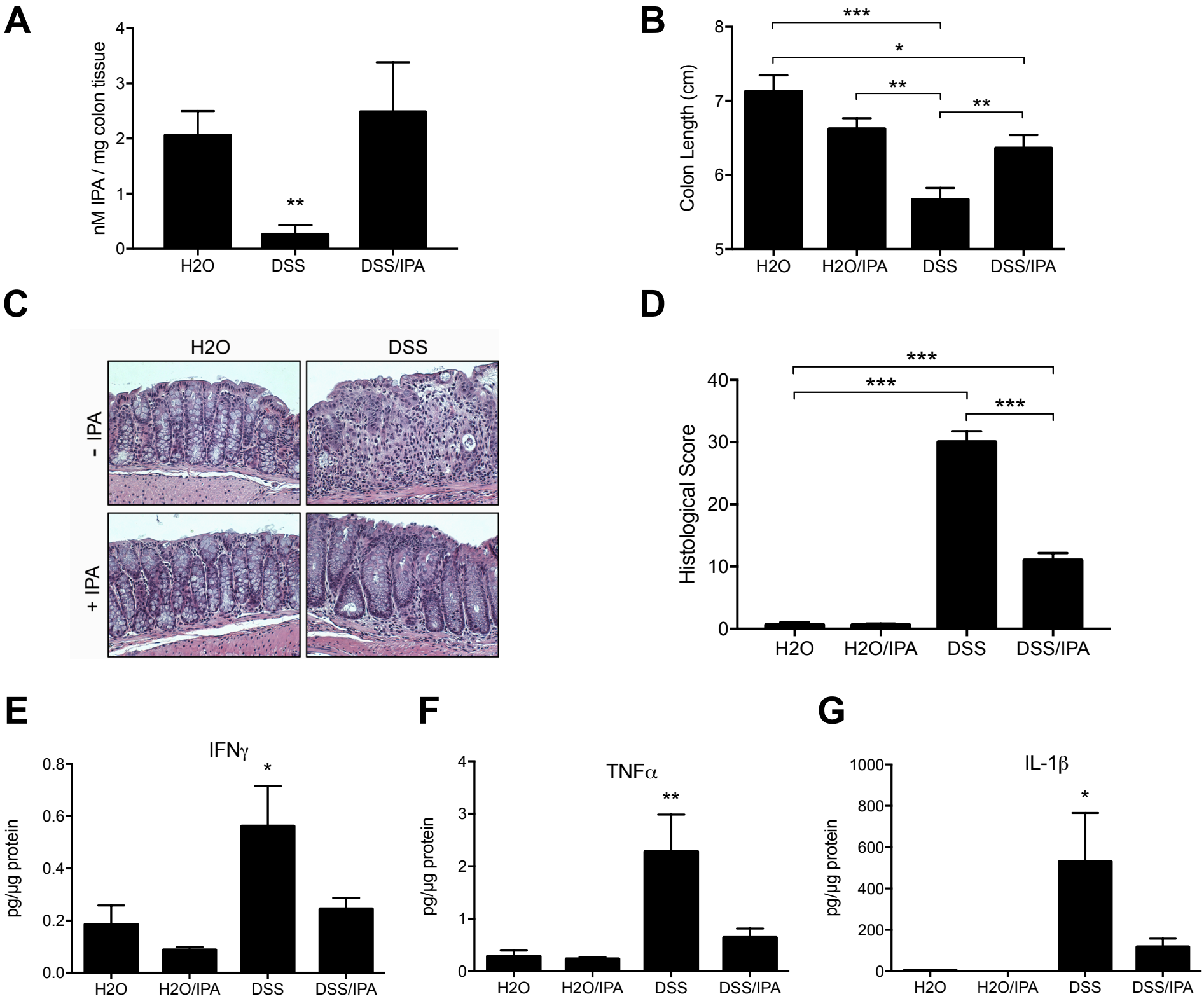
A
nM IPA / mg colon tissue
4
3
2
1
0
**
H2O
DSS
DSS/IPA
B
Colon Length (cm)
8
7
6
5
***
*
**
**
H2O
H2O/IPA
DSS
DSS/IPA
C
H2O
DSS
- IPA
+ IPA
D
Histological Score
40
30
20
10
0
***
***
***
H2O
H2O/IPA
DSS
DSS/IPA
E
IFNγ
pg/µg protein
0.8
0.6
0.4
0.2
0.0
*
H2O
H2O/IPA
DSS
DSS/IPA
F
TNFα
pg/µg protein
4
3
2
1
0
**
H2O
H2O/IPA
DSS
DSS/IPA
G
IL-1β
pg/µg protein
1000
800
600
400
200
0
*
H2O
H2O/IPA
DSS
DSS/IPA